A 183 GHz f_τ and 165 GHz $f_{\max}$ Regrown-Emitter DHBT With Abrupt InP Emitter

Dennis W. Scott, *Student Member, IEEE*, Yun Wei, *Member, IEEE*, Yingda Dong, Arthur C. Gossard, *Fellow, IEEE*, and Mark J. Rodwell, *Fellow, IEEE*

***Abstract*—Small-area regrown emitter–base junction InP/InGaAs/InP double heterojunction bipolar transistors (DHBT) using an abrupt InP emitter are presented for the first time. In a device with emitter–base junction area of 0.7×8 μm^2, a maximum 183 GHz f_τ and 165 GHz $f_{\max}$ are exhibited. To our knowledge, this is the highest reported bandwidth for a III-V bipolar transistor utilizing emitter regrowth. The emitter current density is 6×10^5 A/cm^2 at $V_{\mathrm{CE,sat}} = 1.5$ V. The small-signal current gain $h_{21} = 17$, while collector breakdown voltage is near 6 V for the 1500-Å–thick collector. The emitter structure, created by nonselective molecular beam epitaxy regrowth, combines a small-area emitter–base junction and a larger-area extrinsic emitter contact, and is similar in structure to that of a SiGe HBT. The higher f_τ and $f_{\max}$ compared to previously reported devices are achieved by simplified regrowth using an InP emitter and by improvements to the regrowth surface preparation process.**

***Index Terms*—Epitaxial growth, heterojunction bipolar transistor (HBT).**

I. Introduction

HETEROJUNCTION bipolar transistors (HBTs) have applications in analog and digital systems operating near and above 100-GHz clock rates. To achieve such clock rates, the ac current gain, f_τ, and the power gain, $f_{\max}$, cutoff frequencies must be several hundred GHz. HBTs achieve high f_τ by reducing epitaxial base and collector thickness to reduce transit times. Simultaneous lateral scaling and reduced contact resistances are also required to reduce capacitive charging delays in both f_τ and $f_{\max}$ [1], [2]. Recent examples of epitaxial and lateral scaling in InP mesa DHBTs include 370 GHz f_τ and 459 GHz $f_{\max}$ with 0.6×7 μm^2 emitter–base junction area [3] and 347 GHz f_τ and 492 GHz $f_{\max}$ with 0.6×5 μm^2 emitter junction [4].

SiGe-based HBTs employ superior fabrication techniques to obtain deep-submicrometer features in a planar process. Silicon fabrication technology and silicon bipolar device structures allow for extreme levels of parasitic reduction in SiGe-based HBTs compared to III-V HBTs. This allows SiGe-based HBTs to remain competitive despite the material property advantages of III-V semiconductors. A report of SiGe HBTs with 0.12×2.5 μm^2 emitter–base junctions demonstrates f_τ as high as 350 GHz and simultaneous f_τ and $f_{\max}$ of 270 and 260 GHz, respectively [5]. The junction is obtained by chemical vapor deposition (CVD) of heavily doped polysilicon emitter contact material into a smaller-area aperture, and diffusion is used to form the emitter–base junction. The simultaneous formation of a large contact area and a small-area junction produces a deep-submicrometer emitter–base structure with low emitter access resistance.

We find that conventional III-V HBT emitter–base junction fabrication processes employing mesa etch and self-aligned metal liftoff produce low yield and high emitter access resistance as the emitter mesa and contact dimensions are reduced to deep-submicrometer scales. In SiGe HBTs, large emitter contacts are formed using low resistance polysilicon as the extrinsic emitter contact. In previous reports, we propose a III-V HBT structure utilizing MBE regrowth to form a small-area emitter–base junction and a large, low-resistance emitter contact analogous to SiGe HBT device structures [6], [7]. Others have also proposed regrown emitter HBTs using *selective epitaxy*, which does not form a large extrinsic emitter contact [8]–[10]. In our first account of small-area devices, we report a 160 GHz f_τ and 140 GHz $f_{\max}$ for a graded emitter–base junction InAlAs/InGaAs/InP DHBT [11]. That device had an emitter junction area of 0.7×8 μm^2 and a chirped superlattice (CSL) grade at the emitter–base interface. In this letter, we describe an abrupt emitter–base junction device with an InP emitter. We have eliminated the multiple junctions of the CSL and dramatically improved the regrowth surface preparation process. In doing so, we demonstrate an InP-based regrown emitter HBT with a maximum f_τ of 183 GHz and $f_{\max}$ of 165 GHz. The device has a small-signal current gain h_{21} of 17, and the collector breakdown voltage V_{CEO} is approximately 6 V.

II. Device Structure and Fabrication

Fig. 1 shows a schematic cross section of the regrown-emitter DHBT fabrication process. The device is fabricated using a patterned base–collector template onto which the emitter and cap layers are regrown. The template is grown on a semi-insulating (100) InP substrate. The epitaxial structure is composed of a 3000/100 Å InP/InGaAs n+ subcollector, 1100 Å n- InP collector, 400 Å n- grade and undoped setback layer, 400 Å p+ InGaAs base, a 20 Å InP p-type etch stop, and a 500 Å p+ InGaAs base contact layer. N-type layers are silicon doped, the InGaAs base layers are carbon doped, and the p-type InP is beryllium doped.

Manuscript received March 8, 2004; revised April 9, 2004. This work is supported in part by Defense Advanced Research Projects Agency (DARPA) under Contract N66001-02-C-8080 and in part by Office of Naval Research (ONR) under Contract N0014-99-1-0041. The review of this letter was arranged by Editor D. Ritter.

The authors are with the Department of Electrical and Computer Engineering, University of California, Santa Barbara, CA 93106 USA (e-mail: dennis@umail.ucsb.edu).

Digital Object Identifier 10.1109/LED.2004.829667

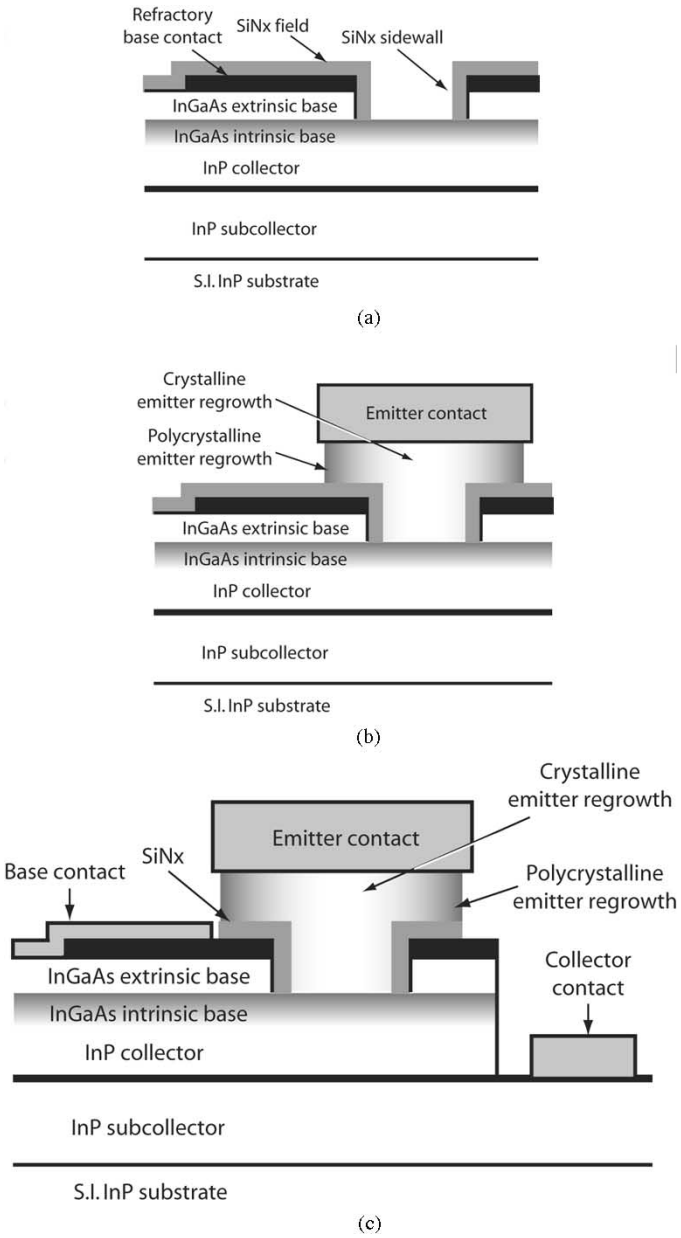

Fig. 1. Cross-sectional schematic of regrown-emitter DHBT fabrication process.

A refractory metal stack is sputtered onto the base–collector template, patterned, and dry etched to form what will be a self-aligned base metal buried under the emitter regrowth. Sputtered SiN_X is then deposited over the entire wafer, and emitter-etch windows are lithographically defined in the centers of the refractory base contacts. Various submicron emitter widths are included on the mask, and the lengths are oriented perpendicular to the [011] direction. Using the single lithography as an etch mask, reactive ion etch (RIE) is used to remove the SiN_X and refractory metal layers from the emitter regrowth areas. After stripping the photoresist and cleaning the wafer of organic material, the base cap layer in the emitter regrowth window is removed using a H_2SO_4-based selective etchant. 1000 Å of plasma-enhanced chemical vapor deposition (PECVD) SiN_X is deposited on the wafer creating an insulative

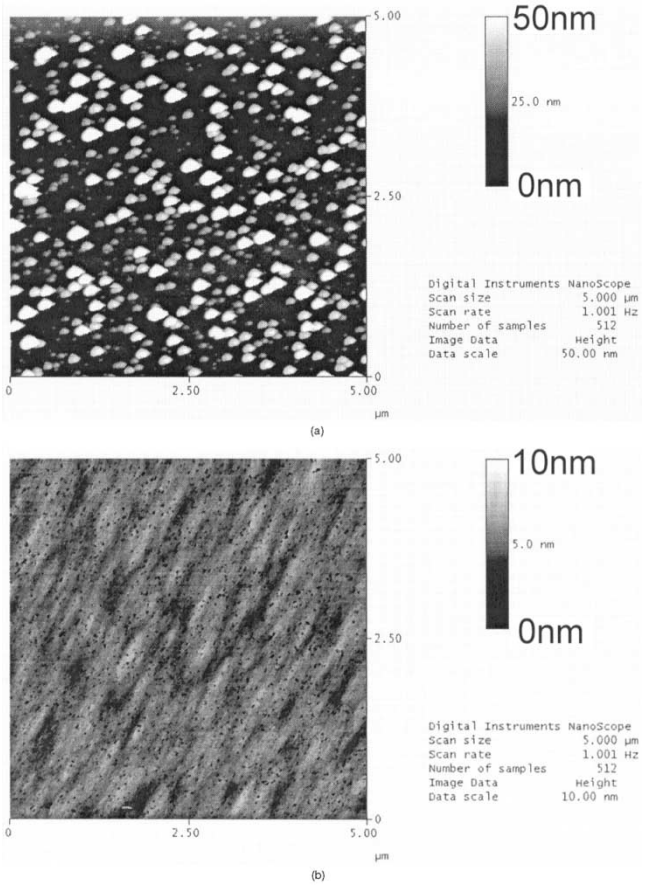

Fig. 2. AFM images of 5 μm^2 regrowth surface prepared by (a) citric acid-based InGaAs etch and HCl-based InP etch producing 50-nm rms roughness and (b) H_2SO_4-based InGaAs etch followed by ozone and HF-based InP etch producing < 10 -nm rms roughness.

layer that will be used for the emitter sidewall. Strongly biased, low pressure RIE is used to form the 0.1 μm vertical SiN_X spacer in the emitter window isolating the emitter regrowth from the base contact region. The 20 Å InP etch stop is removed by a series of ozone treatments and dilute HF-based etchants to expose the intrinsic base regrowth surface. A schematic of the base–collector template before regrowth is shown in Fig. 1(a). The InP emitter structure is regrown by MBE. The emitter region is composed of lightly-doped InP followed by heavily-doped InP and InGaAs. The growth is graded in four steps from the InP lattice-matched InGaAs to a 1500 Å layer of low-resistance InAs contact material. The regrowth on the exposed base material is crystalline while that deposited on SiN_X is polycrystalline. Ti/Pt/Au/Pt metal is deposited over the emitter regrowth windows to form the emitter contacts. The excess regrown material with SiN_X underneath is dry-etched by inductively coupled plasma (ICP) and RIE, respectively, using the emitter metal as an etch mask as shown in Fig. 1(b). Because the base refractory metal has low electrical conductivity, self-aligned Ti/Pd/Au metal is deposited onto the exposed portions of the refractory contacts to reduce feed resistance. Remaining fabrication processes include device isolation and collector contact deposition as shown in Fig. 1(c). Polyimide is used as an insulating material, and a single metal layer forms the device interconnects.

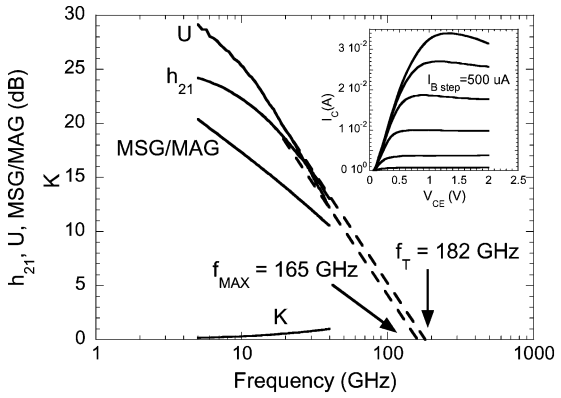

Fig. 3. RF gains and stability factor for $A_E = 0.7 \times 8\ \mu\text{m}^2$ device; inset of common-emitter *I–V* curve with $I_{\text{Bstep}} = 500\ \mu\text{A}$, $h_{21} = 17$.

The single InP layer abrupt emitter used in this device eliminates the 18-layer CSL grade from the InGaAs base to InAlAs emitter used in [11]. We find InP regrowth to be less prone than InGaAs or InAlAs to three-dimensional surface reconstruction, and the elimination of the ternary superlattice makes the regrowth less sensitive to composition and planarity effects. Additionally, the regrowth surface is greatly improved by altering the wet etch chemistry in the pre-regrowth process. As shown in the atomic force microscopy (AFM) image of Fig. 2(a), the citric acid-based InGaAs etch and strong HCl InP etch used in [11] produces a 50-nm root mean square (rms) roughness at the emitter regrowth surface. The AFM image in Fig. 2(b) shows that the H_2SO_4-based InGaAs etch followed by an ozone and weak HCl InP etch used for the present device produces an rms roughness < 10 nm. The simplified growth structure and the improved regrowth surface show dramatic improvement in large-area diode characteristics and in the reflection-high energy electron diffraction (RHEED) patterns during emitter regrowth. Details of these improvements are presented elsewhere [12].

III. Results

The common-emitter current–voltage (*I–V*) curves for the $0.7 \times 8\ \mu\text{m}^2$ device are inset in Fig. 3. The device geometry is identical to that described in [11], and the base–collector layer structure is similar to that of [3] enabling a maximum emitter current density of $6 \times 10^5\ \text{A/cm}^2$ at an associated $V_{\text{CE,sat}}$ of 1.5 V and V_{CEO} of 6 V. The current gain h_{21} for this device is 17. While larger $h_{21} = 20$ and $J_E = 8 \times 10^5\ \text{A/cm}^2$ were observed in [11] using an InAlAs emitter and CSL grade, we do not believe the lower values in this work are caused by the InP emitter. We believe the difference to be an artifact of post-regrowth device fabrication problems and not the abrupt emitter design as we have demonstrated similar InP emitters in other works [3], [13] and do not observe lower values compared to InAlAs emitters. The microwave performance of the device was characterized by S-parameter measurements from 5 to 40 GHz. Simultaneous maximum 183 GHz f_τ and 165 GHz $f_{\max}$ are extracted using -20 dB/dec extrapolations from h_{21} and Mason's Gain as shown in Fig. 3. The RF measurements shown in the figure are obtained at a bias current density of $3 \times 10^5\ \text{A/cm}^2$ and V_{CE} of 1.5 V. Also shown are maximum stable/available power gain (MSG/MAG) and stability factor (K). The observed f_τ and $f_{\max}$ are lower than expected due to passivation of the carbon base doping by hydrogen released during MBE regrowth from the PECVD SiN_X sidewall layer, and due to breaks in the regrown layers arising from both defects in the regrowth window SiN_X sidewall and due to suspected facet-dependence in the emitter growth.

In summary, the first regrown emitter HBT with an InP emitter has been demonstrated. Improvements in performance compared to [11] are due to improvements in the preregrowth process and the simplified epitaxial structure. This abrupt InP emitter device produces the highest reported rf results in a III-V regrown emitter–base HBT.

References

[1] M. J. W. Rodwell, M. Urteaga, Y. Betser, D. Scott, M. Dahlstrom, S. Lee, S. Krishnan, T. Mathew, S. Jaganathan, Y. Wei, D. Mensa, J. Guthrie, R. Pullela, Q. Lee, B. Agarwal, U. Bhattacharya, and S. Long, "Scaling of InGaAs/InAlAs HBTs for high speed mixed-signal and mm-wave ICs," *Int. J. High Speed Electron. Syst.*, vol. 11, no. 1, pp. 159–215, 2001.

[2] M. J. W. Rodwell, M. Urteaga, T. Mathew, D. Scott, D. Mensa, Q. Lee, J. Guthrie, Y. Betser, S. C. Martin, R. P. Smith, S. Jaganathan, S. Krishnan, S. I. Long, R. Pullela, B. Agarwal, U. Bhattacharya, L. Samoska, and M. Dahlstrom, "Submicrometer scaling of heterojunction bipolar transistors," *IEEE Trans. Electron Devices*, vol. 48, pp. 2606–2624, Dec. 2001.

[3] Z. Griffith, M. Dahlström, M. Urteaga, M. J. W. Rodwell, X.-M. Fang, D. Lubyshev, Y. Wu, J. M. Fastenau, and W. K. Liu, "InGaAs/InP mesa DHBTs with simultaneously high f_t and $f_{\max}$, and low C_{cb}/I_c ratio," *IEEE Electron Device Lett.*, vol. 25, pp. 250–252, 2004.

[4] M. Ida, K. Kurishima, K. Ishii, and N. Wantanabe, "High-speed InP/InGaAs DHBTs with thing pseudomorphic base," in *IEEE GaAs IC Symp. Tech. Dig.*, 2003, pp. 211–214.

[5] J.-S. Rieh, B. Jagannathan, H. Chen, K. T. Schonenberg, D. Angell, A. Chinthakindi, J. Florkey, F. Golan, D. Greenberg, S.-J. Jeng, M. Khater, F. Pagette, C. Schnabel, P. Smith, A. Stricker, K. Vaed, R. Volant, D. Ahlgren, G. Freeman, K. K. Stein, and S. Subbanna, "SiGe HBTs with cut-off frequency of 350 GHz," in *IEDM Tech. Dig.*, 2002, pp. 771–774.

[6] D. Scott, H. Xing, S. Krishnan, M. Urteaga, N. Parthasarathy, and M. Rodwell, "InAlAs/InGaAs/InP DHBTs with polycrystalline InAs extrinsic emitter regrowth," in *Proc. IEEE Device Research Conf.*, 2002, pp. 171–172.

[7] D. Scott, C. Kadow, Y. Dong, Y. Wei, A. C. Gossard, and M. J. Rodwell, "Low-resistance n-type polycrystalline InAs grown by molecular beam epitaxy," *J. Cryst. Growth*, to be published.

[8] S. H. Park, T. P. Chin, S. L. Fu, Q. Z. Liu, P. K. L. Yu, T. Nakamura, and P. M. Asbeck, "Sub-micron self-aligned HBTs by selective emitter regrowth," *IEEE Electron Device Lett.*, vol. 19, pp. 121–123, Apr. 1998.

[9] S.-L. Fu, S. H. Park, Y. M. Shin, M. C. Ho, T. P. Chin, P. K. L. Yu, C. W. Tu, and P. M. Asbeck, "GaInP/GaAs HBTs with selectively regrown emitter and wide bandgap extrinsic base," in *Proc. IEEE Device Research Conf.*, June 1994, pp. 91–92.

[10] P. M. Enquist, D. B. Slater, J. A. Hutchby Jr., A. S. Morris, and R. J. Trew, "Self-aligned AlGaAs/GaAs HBT with selectively regrown OMVPE emitter," *IEEE Electron Device Lett.*, vol. 14, pp. 295–297, June 1993.

[11] Y. Wei, D. W. Scott, Y. Dong, A. C. Gossard, and M. J. Rodwell, "A 160 GHz f_T and 140 GHz $f_{\max}$ submicrometer InP DHBT in MBE regrown-emitter technology," *IEEE Electron Device Lett.*, vol. 25, pp. 232–234, May 2004.

[12] D. W. Scott, Y. Wei, M. Urteaga, and M. J. W. Rodwell, "RF performance and process development of InP DHBTs using nonselective emitter regrowth," presented at the Proc. 2004 IEEE Int. Conf. Indium Phosphide Related Materials, Kagoshima, Japan, May 3–June 5 2004.

[13] M. Dahlström, Z. Griffith, M. Urteaga, and M. J. W. Rodwell, "InGaAs/InP DHBTs with > 370 GHz f_t and $f_{\max}$ using a graded carbon-doped base," in *Proc. IEEE Device Research Conf.*, 2003, pp. 6–7.